

# TECHNOLOGY OF GLASS, CERAMIC, OR GLASS-CERAMIC TO METAL SEALING

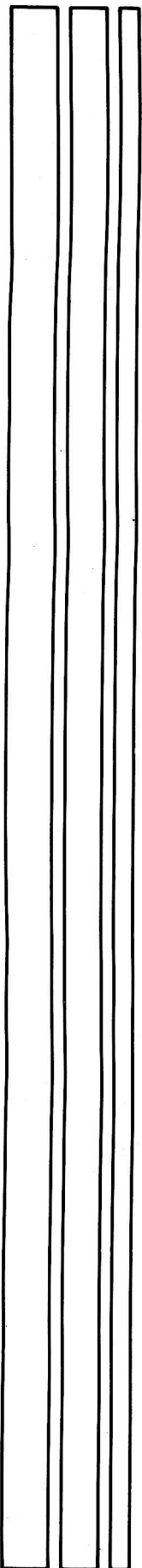
edited by

W. E. MODDEMAN

C. W. MERTEN

D. P. KRAMER





# TECHNOLOGY OF GLASS, CERAMIC, OR GLASS-CERAMIC TO METAL SEALING

*presented at*

THE WINTER ANNUAL MEETING OF  
THE AMERICAN SOCIETY OF MECHANICAL ENGINEERS  
BOSTON, MASSACHUSETTS  
DECEMBER 13-18, 1987

*sponsored by*

THE MATERIALS DIVISION, ASME

*edited by*

W. E. MODDEMAN  
MONSANTO RESEARCH CORPORATION

C. W. MERTEN  
MONSANTO RESEARCH CORPORATION

D. P. KRAMER  
EG&G ELECTRONIC COMPONENTS

Library of Congress Catalog Card Number 87-73098

Statement from By-Laws: The Society shall not be responsible for statements or opinions advanced in papers . . . or printed in its publications (7.1.3)

Any paper from this volume may be reproduced without written permission as long as the authors and publisher are acknowledged.

Copyright ©1987 by  
THE AMERICAN SOCIETY OF MECHANICAL ENGINEERS  
All Rights Reserved  
Printed in U.S.A.

## PREFACE

The classes of materials known as glasses and ceramics possess certain properties which make their use in engineering applications attractive. Both have high compressive strength and low electrical conductivity, and both are resistant to chemical attack. Ceramics retain their strength at high temperatures and are resistant to creep at these temperatures. They are also stronger than glasses. However, fabrication of nonolithic ceramic components is a complex process which requires sizing and pressing of powders, sintering, and machining of complex shapes. Glasses begin to flow at much lower temperatures than ceramics do; therefore, they have the advantage that they can be more easily molded into complex shapes. Glass-ceramics are hybrids of glasses and ceramics produced by precipitating crystalline phases from a glass matrix. Their strengths are higher than those of glasses but they can still flow into their final shape.

The primary drawback to the exclusive use of glasses, ceramics, and glass-ceramics in designs is their brittle mechanical behavior. Compared to metals, all exhibit low fracture toughness and high notch sensitivity. A more rational approach to the use of these materials is to incorporate them into designs only in places in which their properties enhance the performance of the final product. The key problem to the successful application of glasses, ceramics, and glass-ceramics then becomes their joining to dissimilar materials.

This symposium addresses the current technology of bonding metal to glass, ceramic, or glass-ceramic. Two fundamental aspects which are addressed are the microstructural features of bonding at glass-ceramic and ceramic to metal interfaces and the nature of mechanical interactions which occur as a result of bonding between materials with dissimilar mechanical and thermal properties.

W. E. Moddeman  
C. W. Merten  
D. P. Kramer



## CONTENTS

Chemical Bonding at Glass-To-Metal Interfaces <i>J. A. Pask</i> . . . . .	1
Properties of Seals Made With $\text{Li}_2\text{O-A1}_2\text{-SiO}_2$ -Glass Ceramics and Aluminum-Containing Austenitic Stainless Steels <i>R. T. Cassidy and P. N. Fagin</i> . . . . .	9
Improved Glass-Ceramic to Metal Seals in Actuator and Detonator Applications With an Aluminum-Containing Austenitic Stainless Steel <i>J. C. Birkbeck, R. T. Cassidy, P. N. Fagin, and W. E. Moddeman</i> . . . . .	15
Reactions and Bonding Between Glasses and Titanium <i>R. K. Brow and R. D. Watkins</i> . . . . .	25
Processing of Glass to Aluminum Seals Via an Injection Molding Technique <i>D. P. Kramer, R. T. Massey, and D. L. Halcomb</i> . . . . .	31
Processing and Interfacial Analysis of Glass-Ceramic to Metal Seals <i>R. E. Loehman</i> . . . . .	39
Analysis of End Stresses in Glass-Metal Bimaterial Strips <i>F. P. Gerstle, Jr. and R. S. Chambers</i> . . . . .	47
Stress Analysis of Header Material Sets <i>C. M. Woods and C. W. Merten</i> . . . . .	61
Diffusion Zone Model of a Ceramic/Metal Interface <i>F. Delale</i> . . . . .	69
A Review of the Mechanical Testing of the Coating-Substrate Bond Strength in Ceramic-Metal Systems <i>B. A. Chapman, H. D. DeFord, G. P. Wirtz, and S. D. Brown</i> . . . . .	77
Interfacial Mechanics of Seals <i>C. W. Lau, A. Rahman, and F. Delale</i> . . . . .	89

## CHEMICAL BONDING AT GLASS-TO-METAL INTERFACES

J. A. Pask

Material and Chemical Sciences Division

Lawrence Berkeley Laboratory

and

Department of Materials Science and Mineral Engineering

University of California

Berkeley, California

### ABSTRACT

Chemical bonding is attained at a glass-to-metal seal when stable chemical equilibrium is obtained at the interface. Equilibrium is reached by saturating the interfacial zone with the oxide of the substrate by redox reactions at the interface between the glass and metal, or by applying the glass to a preoxidized metal at temperature. Under these conditions an oxide layer is present at the interface. It is compatible with both the metal and glass and provides the chemical bonding.

### Introduction

Glass-to-metal seals are made at sufficiently high temperatures for the glass to behave as a highly viscous liquid and to undergo the necessary chemical reactions with the metal. Satisfactory adherence from an engineering point of view is dependent on chemical bonding and a favorable stress pattern at the interface [1,2]. The strongest seals require a chemical bond, especially if they have to be vacuum-tight or impermeable to liquids. This presentation is a tutorial overview of the factors playing a role in chemical bonding at glass-to-metal interfaces based on our current understanding as to how and why such a phenomena can be achieved. The intention is to show that the principles and basic requirements are the same for all seals regardless of their complexity.

With regard to physical requirements it will suffice to emphasize the importance of having favorable stress gradients in the interfacial zones. The need for matching the coefficients of thermal expansion so that the glass is in slight compression is well recognized (3,4,5). However, the dependence of stress gradients on composition gradients and microstructures that develop during the making of the seals is not as well recognized and will be pointed out later.

### Chemical Bonding at Interfaces

Chemical bonding is exemplified by a continuous electronic structure across the interface represented by metallic, ionic and covalent types of bonding, and not by van der Waals attractive forces. Continuity is achieved by a balance of bond energies which in turn requires stable chemical equilibrium between the two phases only at the interface. Equilibrium implies that no driving force for chemical reactions exists at elevated temperatures. If equilibrium did not exist, there would be a thermodynamic driving force for a potential reaction at the interface. The significance of the reaction is that it is occurring because the system is changing towards stable chemical equilibrium. As a caution, however, it should be pointed out that the expected reaction sometimes may not occur because of some barrier such as a high activation energy or the presence of contamination, resulting in metastable chemical equilibrium which results in van der Waals bonding and not chemical bonding.

Another aspect of achieving equilibrium at the interface is that the reacting phases must be compatible. At metal/metal and ceramic/ceramic interfaces either solution or compound formation take place readily because in each case the phases are compatible in the sense that no valence changes occur during the reaction. The simplest reaction is solution of one phase by the other to form an immediate equilibrium saturation at the interface. A continuation of the reaction is associated with diffusion into the bulk which is slower than the reaction itself. Equilibrium is thus maintained at the interface. This process is generally referred to as diffusion bonding.

Glass-to-metal interfaces, however, are not compatible in this sense. Reactions that occur at

the interface are of the redox type involving an oxidation of metal atoms and a reduction of cations in the glass. In the case of an oxide glass, the oxygen released by the reduction of a cation forms an oxide with the metal atom at the interface. Saturation of the interfacial zone with the metal oxide and the presence of a molecular or multimolecular layer of oxide results in equilibrium and chemical bonding at the interface since the metal oxide layer is compatible with both its metal and the glass. In practice, the necessary compatible oxide layer at the interface is obtained by preoxidizing the metal, which also is a redox reaction. The oxide undergoes a controlled solution by the applied glass.

These requirements for chemical bonding are schematically illustrated in Fig. 1. The first line represents a cross-section with a partially dissolved metal oxide layer and the adjoining metal and glass interfaces saturated with the metal oxide resulting in the formation of electronic structures (chemical bonding) across the interfaces. With this structure the assembly would be affected by the physical properties of the oxide. The second line illustrates a case in which the glass has dissolved all of the oxide except one layer at the interface. The bonding requirements are still fulfilled. The overall properties of the assembly will, however, not be affected by the presence of a discrete oxide layer but will be by the resulting thicker composition gradient into the glass formed by solution/diffusion. Lastly, the third line illustrates the case in which the interface is not saturated with the metal oxide. Under this condition the electronic structure across the interface is lost because of a lack of balance of bond energies with the formation of van der Waals bonding. Separation or cracking along the interface can then occur with the application of stresses.

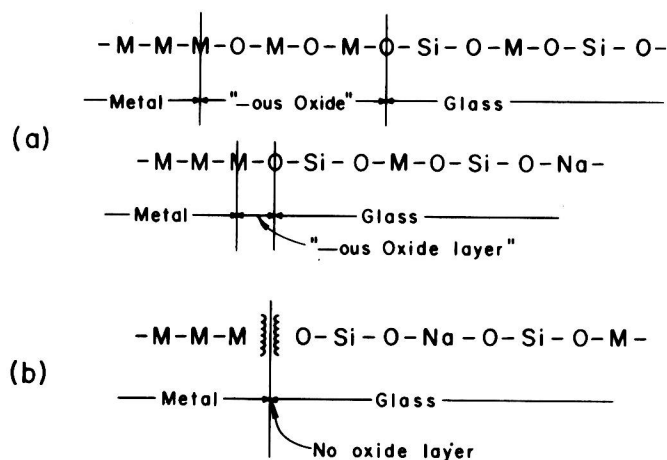


Fig. 1. Schematic of bonding of phases at interfaces: (a) chemical bonding (continuous electronic structure) when glass and metal at interface saturated with Metal oxide (MO), and (b) van der Waals bonding (no electronic structure across interface).

From the thermodynamic viewpoint, in the first two cases the activity of the metal oxide due to its presence is one. It is thus also one at the metal/oxide and oxide/glass interfaces. In the third case, the metal oxide activities are equal in the two phases at the interface but are less than one. Activity of one is required for chemical bonding.

The processing requirements for the achievement of chemical bonding are (a) the formation of a continuous intimate interface by wetting of liquid glass on the metal at the sealing temperature, and (b) the presence of stable chemical equilibrium at the interface.

### Wetting and Spreading

The formation of an intimate or true interface of molten glass on an uncontaminated pristine metal or clean preoxidized surface at elevated temperatures is necessary to initiate reactions at the interface. Wetting is also necessary to have the molten glass continuously distribute itself over the metal surface of the assembly and penetrate surface irregularities.

Sessile drop experiments, with proper interpretation, are thus important because they provide information on the formation of interfaces and the existence of reactions at the interfaces which normally may not be recognized and overlooked. It is thus worthwhile to examine and understand the associated principles.

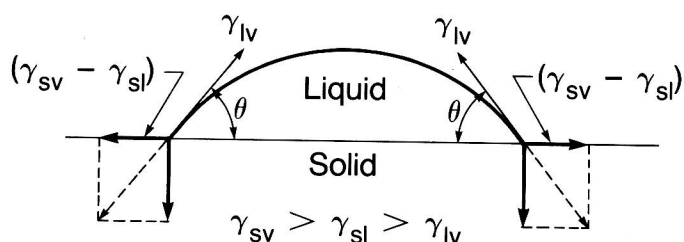
Sketches of cross-section planes perpendicular to the interfaces and passing through the vertical axes of both wetting and non-wetting sessile drops are shown in Fig. 2. In each case the configuration is determined by the solid rigid phase and the surface energies of the phases. The relative order of surface energy values is metals > crystal oxides > oxide glasses. Under non-reactive conditions, wetting represented by a steady state acute contact angle ( $\theta < 90^\circ$ ), always occurs when  $\gamma_{sv} > \gamma_{sl} > \gamma_{lv}$  ( $\gamma$  represents interfacial energy: for solid/vapor as sv, solid/liquid as sl, and liquid/vapor as lv). This configuration is typical of a liquid glass drop on a metal substrate. Also under non-reactive conditions, non-wetting, represented by a steady state obtuse contact angle ( $\theta > 90^\circ$ ) always occurs when  $\gamma_{sv} < \gamma_{sl} < \gamma_{lv}$ . This configuration is typical of a liquid metal drop on a ceramic or glass substrate. It should be noted that  $\gamma_{sl}$  in both cases is inbetween  $\gamma_{sv}$  and  $\gamma_{lv}$ , i.e., the higher surface energy is reduced in contact with the lower surface energy phase. Wetting is defined as the reduction of  $\gamma_{sv}$  of the rigid substrate by the liquid. In the case of non-wetting, the surface energy of the rigid substrate is not reduced by the liquid; an intimate interface, however, is formed.

The driving force for wetting is thus  $(\gamma_{sv} - \gamma_{sl})$  which is acting on the periphery of the liquid drop. The resisting force is  $\gamma_{lv}$  since the lowest free energy configuration for the liquid is a sphere. A balance of these forces gives us a steady state contact angle and the familiar Young-Dupré equation:

$$\gamma_{sv} - \gamma_{sl} = \gamma_{lv} \cos \theta \quad (1)$$

In the absence of a reaction, whether stable or metastable chemical equilibrium exists, the driving force for wetting never exceeds  $\gamma_{lv}$  and spreading or dynamic extension of the liquid drop does not occur [6].

### Sessile Drop Configurations



$$\gamma_{sv} - \gamma_{sl} = \gamma_{lv} \cos \theta$$

$$\gamma_{sv} - \left( \gamma_{sl} + \frac{-dG_R}{dA \cdot dt} \right) \rightarrow \gamma_{lv} \cos \theta$$

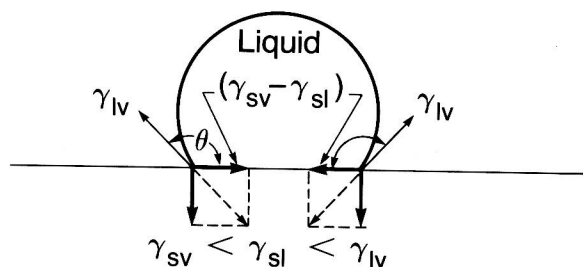


Fig. 2. Sessile drop configuration: (top) wetting, and (bottom) non-wetting. See text for significance of equations.

Examples of the value of understanding the significance of these relationships follows: If  $\gamma_{sv}$  is known to be greater than  $\gamma_{lv}$  but non-wetting is observed, then experimental  $\gamma_{sl}$  must be greater than  $\gamma_{sv}$  and also  $\gamma_{lv}$ . The conclusion is that a true intimate interface between the solid and liquid in question must not have formed due to some unreactive contamination on the solid surface. On the other hand, if  $\theta < 90^\circ$  indicating that  $\gamma_{sl}$  is inbetween  $\gamma_{sv}$ , a wetted true interface is present. Furthermore, if  $\gamma_{lv}$ ,  $\gamma_{sv}$  and  $\gamma_{sl}$  is inbetween them, a true interface is also present but the non-wetting liquid will not penetrate surface irregularities.

When a reaction occurs, the free energy of reaction per unit interfacial area and unit time enhances the driving force for wetting as indicated by the inequality in Fig. 2 only if the solid is an active participant. In a solid state solution reaction, if only one phase is unsaturated relative to the other, the unsaturated or solvent phase is changing its composition and the solute is not. We can then define the solvent as the active participant and the solute as the passive participant. If both phases are unsaturated relative to each other or they form a compound at interface, then both phases are active participants. If the enhanced driving force for wetting exceeds  $\gamma_{lv}$ , then spreading occurs which can happen either when  $\gamma_{sv}$  is greater or smaller than  $\gamma_{lv}$  [17]. The dynamic stage of movement or spreading stops when the liquid is completely reacted.

### Redox Reactions

It has been indicated that chemical bonding at glass-to-metal interfaces is associated with the presence of stable chemical equilibrium. Equilibrium requires the presence of phase compatibility at the interfaces which is achieved by saturating the interfacial zone with a low valent oxide of the substrate metal resulting in a transition layer of the oxide at the interface. This structure or microstructure is realized by redox reactions.

### Preoxidation of Metal

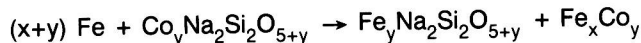
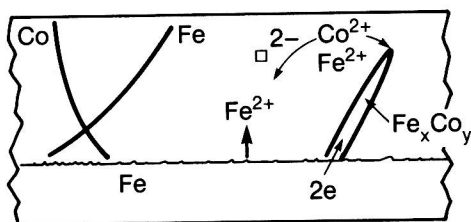
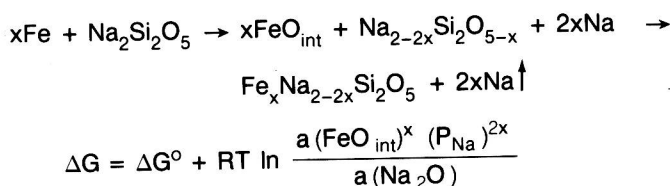
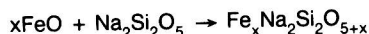
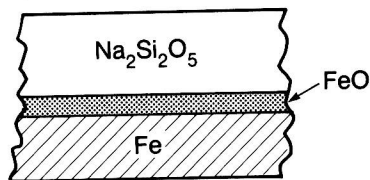
The normal technological procedure of achieving chemical bonding and favorable stress gradients in glass-to-metal assemblies is to preoxidize the metal and apply the glass as shown in the upper sketch of Fig. 3. The model system of  $\text{Na}_2\text{Si}_2\text{O}_5$  glass and Fe metal is being used to provide examples [8,9,10]. At temperature the molten glass wets and dissolves the oxide. The glass at the oxide interface immediately becomes saturated because the solution rate of the oxide is faster than the diffusion rate of the dissolved oxide into the bulk glass. Chemical bonding at the interface is thus realized. The oxide layer also bonds chemically to the metal which is saturated with the oxide, at least at the surfaces. The saturated interfaces and the oxide layer thus have a chemical activity of one for  $\text{Fe}_x\text{O}$ , which is a requirement for chemical bonding in this case.

As the dissolved oxide diffuses into the glass a concentration gradient is formed as schematically shown in the upper sketch of Fig. 4. It can be seen that, as the oxide dissolves, the concentration gradients become more extended, but the equilibrium saturation at the oxide/glass interface and consequently bonding are always maintained because of the faster solution rate. Such an addition of a metal oxide to the glass affects its coefficient of expansion because of an increase of its O/Si ratio and introduction of cations with different degree of covalency. Concentration gradients, then are proportional to thermal expansion coefficient gradients which generally result in more favorable stress gradients [11]. It can be seen that the composition gradients become more extensive with increasing



thicknesses of starting oxide. It is thus evident that many, if not most, experiments based on varying thicknesses of oxide which were presumably done to improve chemical bonding were actually strengthening the assembly by realizing more favorable stress gradients, similar to a graded seal.

### Solution of Oxide



### Micro-galvanic cell in the interfacial zone

Fig. 3. Schematic cross-sections of (top) glass on preoxidized metal with equation representing solution reaction of oxide by glass, (middle) two step equation representing redox reaction of glass on metal - formation of metal oxide at interface followed by solution of oxide in glass, and free energy equation for first step, and (bottom) equation for redox reaction of glass containing CoO with Fe substrate resulting in indicated  $\text{Co}^{2+}$  and  $\text{Fe}^{2+}$  gradients - formation of  $\text{Fe}_x\text{Co}_y$  dendrites by microgalvanic cell mechanism with electronic circuit of electrons and negative vacancies. Standard free energies negative except for first step of middle equation.

### Non-spontaneous Metal/Glass Redox Reactions

When an oxide layer is dissolved completely, the oxide saturation at the interface is lost as the diffusion of the dissolved oxide continues into the glass (lower sketch of Fig. 4). At this point, because of the loss of chemical equilibrium, redox reactions become possible as illustrated by the equations in the middle of Fig. 3 for the model system of  $\text{Na}_2\text{Si}_2\text{O}_5$  glass and Fe metal. The same basic relationship exists if the glass is applied to an unoxidized metal. The net reaction (Eq. 4) consists of two step reactions: the formation of the metal oxide at the interface (Eq. 2) followed by its solution by the glass (Eq. 3).

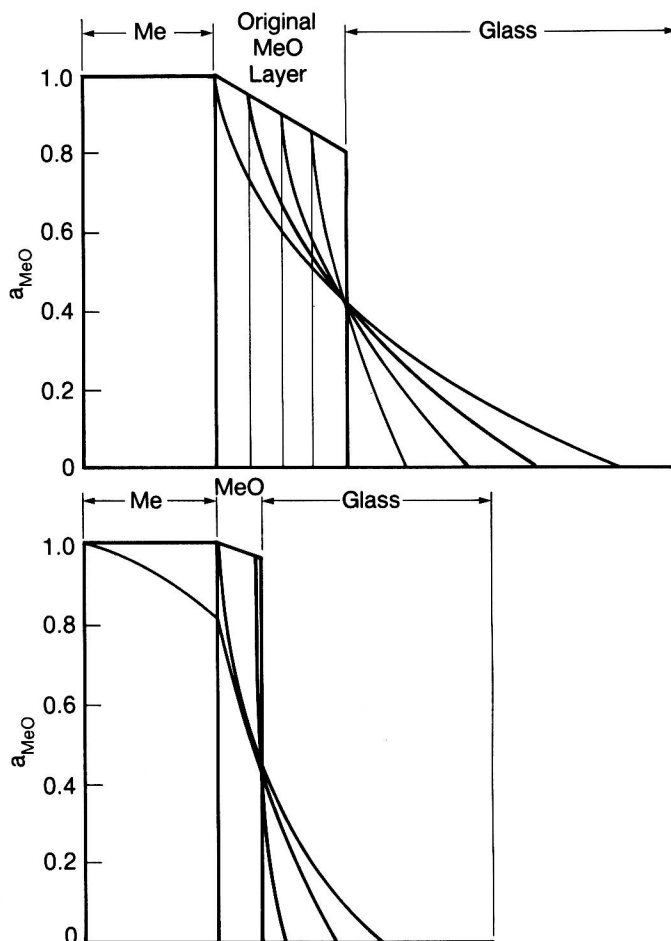
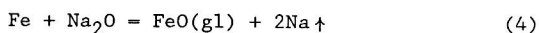
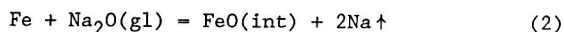


Fig. 4. Schematic showing lengthening activity gradients of MeO in glass with continuing solution of oxide by glass. (top) Gradient extension proportional to thickness of oxide by glass. (bottom) Loss of saturation at interface with continued heating beyond complete solution of oxide layer.



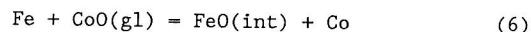
$$\Delta G = \Delta G^\circ + RT \ln \frac{a(\text{FeO})_{\text{int}} \cdot p(\text{Na})^2}{a(\text{Fe}) \cdot a(\text{Na}_2\text{O})_{\text{gl}}} \quad (5)$$

The first step of this reaction at the sealing temperature of 1000°C, however, does not take place spontaneously ( $\Delta G$  is positive) since its  $\Delta G^\circ$  under standard conditions is positive, because no cation in this glass has an oxidation potential less than that of the substrate atom. The conditions, other than standard, under which  $\Delta G$  for this reaction becomes negative are determined by its equilibrium constant  $K$ , or activity quotient, shown in the free energy equation Eq. 5, and in Fig. 3. The activity quotient has to be sufficiently smaller than unity for the overall term to be more negative than the positive  $\Delta G^\circ$ . The reaction is thus favored with a low  $p(\text{Na})$ , a low activity of  $\text{FeO}(\text{int})$ , and high  $a(\text{Na}_2\text{O})_{\text{gl}}$ . The  $a(\text{Fe})$  is close to one and can be neglected. The pressure of the formed Na vapor has to exceed ambient pressure to nucleate bubbles of Na vapor at the interface and escape; therefore, this reaction is potentially more favorable in a dynamic vacuum or a low pressure ambient atmosphere. The loss of Na results in a weight loss that could be monitored for analysis of the kinetics of the reaction. The  $a(\text{Na}_2\text{O})$  in the glass is dependent on the glass composition, i.e., the availability of  $\text{Na}_2\text{O}$  for reaction. Experimentally, this requirement is fulfilled by  $\text{Na}_2\text{Si}_2\text{O}_5$  glass. The  $a(\text{FeO})$  at the interface of Fe surface is dependent on the  $p(\text{O}_2)$  in the ambient atmosphere and the amount of dissolved FeO in the starting Fe. Above the dissociation  $p(\text{O}_2)$  for FeO of  $1.2 \times 10^{-15}$  atm, the surface remains covered with FeO and the  $a(\text{FeO})_{\text{int}}$  is one. Below the dissociation  $p(\text{O}_2)$  bulk oxide does not form and any oxide that may have been present on the surface dissociates with a decrease of  $a(\text{FeO})_{\text{int}}$  below one. It is necessary to consider the step reactions in order to fully understand the nature of the net reaction and to correctly interpret the kinetics. This requirement exists because the second step reaction has a negative  $\Delta G^\circ$  and thus occurs spontaneously.

It is important to be aware of these reactions because of their possible occurrence as complicating reactions. In practice, however, it is more convenient to have compositions that lead to spontaneous redox reactions under regular processing conditions, generally in atmospheric air.

#### Spontaneous Metal/Glass Redox Reactions

The porcelain enamel technologists of many generations ago, however, experimentally found that a small addition of CoO to the enamel glass caused a spontaneous redox reaction with the substrate metal when all of the surfacer oxide was dissolved, without changing firing conditions. The existing surface metal oxide was formed either by preoxidation or during the initial stages of heating before the applied glass particles flowed.



The  $\Delta G^\circ$  change for this reaction is negative because CoO in the glass is easily reduced by Fe which has a higher oxidation potential than Co (i.e.,  $\text{Co}^{2+} = -0.28$  eV vs.  $\text{Fe}^{2+} = -0.44$  eV). Within normal experimental conditions  $\Delta G$  remains negative even though the  $a(\text{FeO})$  in the Fe substrate and interface may be one. The FeO that is introduced into the glass by either redox reaction maintains the glass/metal interface saturated with the oxide which is necessary to maintain chemical bonding. A contributing factor to a negative  $\Delta G^\circ$  is the energy gain due to the fact that Co readily alloys with Fe [12,13]. This alloying tendency results in the establishment of micorgalvanic cells which cause the formation of  $\text{FeCo}_x$  dendrites in the glass in the interfacial zone, as indicated in the lower sketch of Fig. 3.

This reaction, plus the corrosion of the metal interface, leads to the development of a composite-type microstructure which increases the strength of the assembly. An example of this type of microstructure is shown in Fig. 5, which pictures the interfacial zone of Cr and  $\text{Na}_2\text{Si}_2\text{O}_5$ .

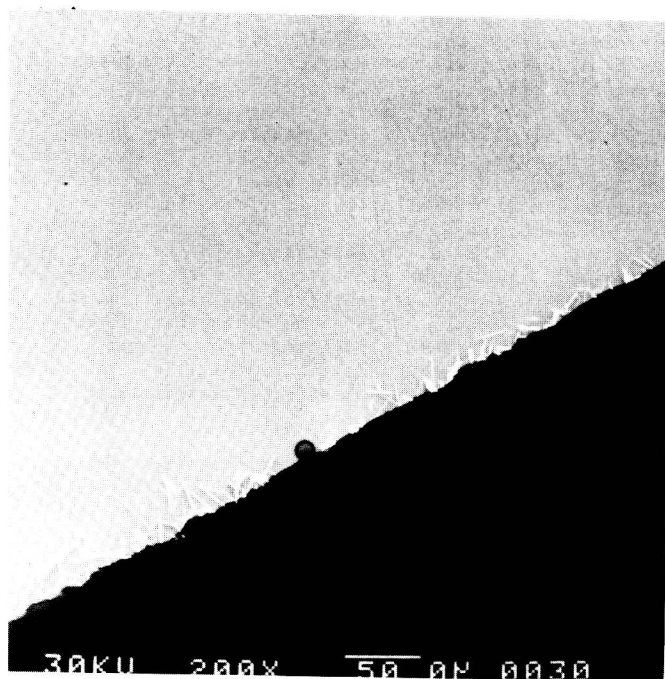


Fig. 5. SEM photograph of cross-section of interfacial zone for Cr and glass showing dendritic growth of Cr silicide in the glass at the interface.

Instead of modifying the glass composition in order to realize a favorable, i.e., negative  $\Delta G^\circ$  for a redox reaction under any firing conditions including 1 atm. air, it is possible to use a highly reactive metal as a substrate. Experiments have been made with Cr, Ti and Zr, for example, which have sufficiently high oxidation potentials to even reduce silica in the glass with the formation of an alloy of the metal with Si, or a silicide compound [14,15]. A representative reaction is that of Cr with  $\text{Na}_2\text{Si}_2\text{O}_5$  glass to form platelets and wire-like crystals of  $\text{CrSi}_x$  alloy by means of a microgalvanic cell mechanism similar to that for  $\text{FeCo}_x$  (Fig. 5). The released oxygen formed oxides of the substrate metals. Saturation of the interfacial zone with the substrate oxides results in chemical bonding. When a Ti substrate was used, a silicide compound e.g.,  $\text{Ti}_5\text{Si}_3$  was formed as a layer at the interface instead of an alloy ( $\text{TiSi}_x$ ). In this case, the compound is compatible with the Ti substrate and the glass.

Another type of glass-metal assembly is one in which the substrate metal is an alloy. Because of the differences in the oxidation potentials or reactivities of the components of the alloys, the redox reactions are not stoichiometric whether the alloy is exposed to atmospheric oxidation, or reacts directly with the glass. Some recent observations on reactions and bonding of a boro-silicate glass to several  $\text{Ni}_2\text{OCr}$  alloys (one contained ppms of impurities and a second had 2.0 wt. percent of Si as the principal impurity) provide examples of the complexities encountered [16]. On preoxidation, the purer alloy formed a multilayer oxide scale with a NiO-rich outer layer whereas the latter alloy formed a chromium oxide scale containing in solution a NiO concentration gradient from the alloy interface. The type of cross-sectional oxide microstructures formed can be seen in Fig. 6. Stable chemical equilibrium exists at all interfaces. Bonding and strength problems related to scale adherence integrity, however, arise because of physical incompatibilities such as specific volume, epitaxial and coefficient of thermal expansion differences.

With application of the glass, solution reactions occur as discussed before. The presence of any undissolved oxide, or any penetration of a porous oxide layer by the glass, play a significant role in determining the strength and vacuum tightness of the assembly. If all of the oxide is dissolved or if the glass is placed in contact with unoxidized alloy, then redox reactions take place with the glass. With saturation of the glass at the interface, a  $\text{Cr}_2\text{O}_3$  layer forms with the development of chemical bonding as observed in the upper photo of Fig. 6. The ultimate acceptability of the assembly will be determined by the physical factors which will be affected by the concentration gradients and microstructure that develop during the chemical reactions that go on in reaching stable chemical equilibrium in the interfacial zone.

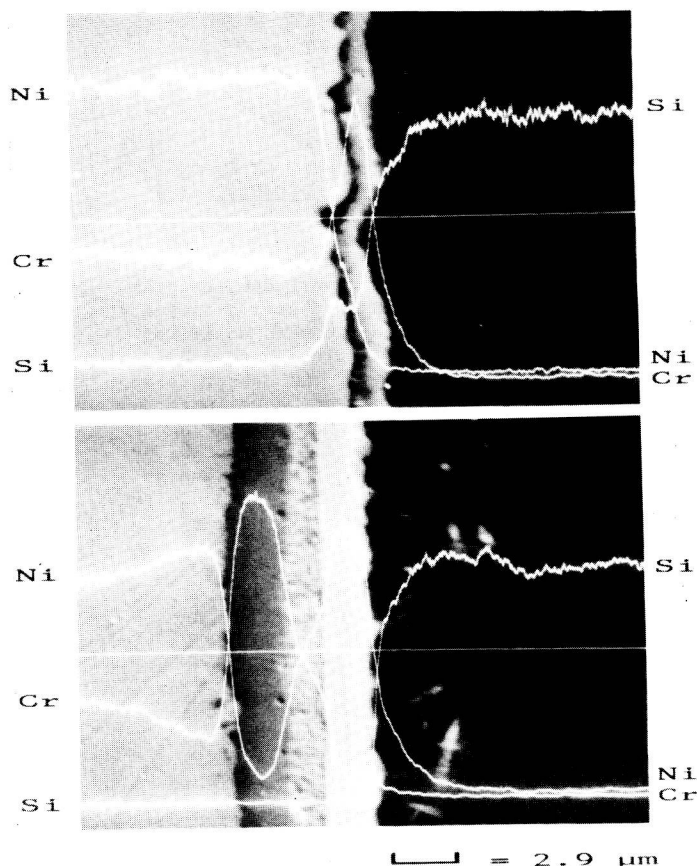


Fig. 6. X-ray line scans for Cr, Ni, and Si across the interfaces of dental porcelain glassy phase (top) on 80Ni20Cr type alloy with Si additive preoxidized 60 min at 1000°C in air. (SEM photos at same magnification, bar = 2 μm).

#### Reactivity of Metals

In making glass-to-metal seals glasses come in contact with the metal substrate after dissolving any existing metal oxide on the substrate. Redox reactions would then be necessary to maintain the interface saturated with the metal oxide. The reaction at the interface will depend on the relative oxidation potentials of the metal and the potentially reducible cations in the glass. The metals can be arbitrarily grouped on the basis of reactivity in vacuum and low  $P(\text{O}_2)$  atmospheres, viz, magnitude of oxidation potential, as low, medium and high.

The low reactivity metals would include Au, Pt and Ag. Oxidation in air does not produce bulk oxides although absorbed layers of the oxide of the metal are formed. Such layers do not form or, if formed, dissociate on heating in normal vacuum and inert atmospheres, i.e., at low  $p(\text{O}_2)$ . On firing metal/glass assemblies in air the layer of oxide is sufficient so that on solution the interfacial zone becomes saturated with the respective substrate

oxide because of the very low solubility and diffusivity of the oxides in glasses. In case of Ag, however, the  $\text{Ag}_2\text{O}$  forms a Ag-silicate at the interface which is compatible with both Ag and the glass saturated with  $\text{Ag}_2\text{O}$ . In all cases chemical bonding occurs. On firing in vacuum, however, no redox reactions occurred at the interfaces of the Au and Pt assemblies resulting in no chemical bonding. Redox reactions, however, formed in the Ag/glass assemblies with the development of chemical bonding [17].

The medium group includes such metals as Fe, Ni and Co. The high reactivity group includes such metals as Cr, Ti and Zr. The general chemical behavior of these types of assemblies have been discussed.

#### Summary

It has been shown that chemical bonding at glass-to-metal seals is achieved when stable chemical equilibrium exists at the interfaces. Compatibility of electronic structures of the two phases is required but not easily acquired because of the incompatibility of the metallic and ionic-covalent bonding. A phase is needed at the interface that is compatible with both the metal and the glass. A low-valent oxide of the metal is such a phase and is obtained by redox reactions. In redox reactions the metal reacts with the glass wherein a metal atom is oxidized and a cation in the glass is reduced releasing oxygen anions that are picked up by the oxidized metal atoms. Continued reaction maintains saturation of the interfacial zone with the forming metal oxide. The degree of reactivity and the complexity of the reactions are determined by the relative oxidation potentials of the various metallic atoms and cations in the glasses. Instead of depending on such redox reactions the usual technological approach is to first preoxidize the metal in air, which is a redox reaction, before applying the glass.

#### Acknowledgment

Grateful acknowledgment is extended to Dr. Antoni P. Tomsia for extensive discussions and preparation of the figures.

#### References

1. A.P. Tomsia and J.A. Pask, "Chemical Reactions and Adherence at Glass/Metal Interfaces: An Analysis," *Dent. Mater.*, 1 [2] 10-16 (1986).
2. M.G. Nicholas and D.A. Mortimer, "Ceramic/Metal Joining for Structural Application," *Mater. Sci. Technol.*, 1 [9] 657-665 (1985).
3. S.M. Rekhson, "Annealing of Glass-to-Metal and Glass-to-Ceramic Seals. Part 1. Theory," *Glass Technol.*, 20 [1] 27-34 (1979).
4. S.M. Rekhson, "Annealing of Glass-to-Metal and Glass-to-Ceramic Seals. Part 2. Experimental," *Glass Technol.*, 20 [4] 132-143 (1979).
5. A.K. Varshneya, "Stresses in Glass-to-Metal Seals," in: *Treatise on Materials Science and Technology*, Vol. 22, 241-306, Academic Press, Inc., (1982).
6. I.A. Aksay, C.E. Hoge and J.A. Pask, "Wetting Under Chemical Equilibrium Conditions," *J. Phys. Chem.* 12 [78] 1178-83 (1974).
7. P.P. Sharps, A.P. Tomsia and J.A. Pask, "Wetting and Spreading in the Cu-Ag System," *Acta Metall.*, 29 [7] 855-865 (1981).
8. A.P. Tomsia and J.A. Pask, "Kinetics of Iron-Sodium Disilicate Reactions and Wetting," *J. Am. Ceram. Soc.*, 64 [9] 523-528 (1981).
9. J.J. Brennan and J.A. Pask, "Effect of Composition on Glass-Metal Interface Reactions and Adherence," *ibid.*, 56 [2] 58-62 (1973).
10. C.E. Hoge, J.J. Brennan and J.A. Pask, "Interfacial Reactions and Wetting Behavior of Glass-Iron Systems," *ibid.*, 56 [2] 51-54 (1973).
11. P. Mayer, J.A. Topping and M.K. Murthy, "Correlation Between Thermal Expansion of Glass and Glass-to-Metal Adherence," *J. Can. Ceram. Soc.*, 43, 43-46 (1974).
12. M.P. Borom and J.A. Pask, "Role of Adherence Oxides in Development of Chemical Bonding at Glass-Metal Interfaces," *J. Am. Ceram. Soc.*, 49 [1] 1-6 (1966).
13. M.P. Borom, J.A. Longwell and J.A. Pask, "Reactions Between Metallic Iron and Cobalt Oxide-Bearing Sodium Disilicate Glass," *ibid.*, 2 [50] 61-66 (1967).
14. J.A. Pask and A.P. Tomsia, "Wetting, Spreading and Reactions at Solid/Liquid Interfaces," in: *Surfaces and Interfaces in Ceramic and Ceramic-Metal Systems*, J.A. Pask and A.G. Evans Eds., Plenum Publishing Corporation, pp. 411-419, 1981.
15. A.P. Tomsia, F. Zhang and J.A. Pask, "Reactions and Bonding of Sodium Disilicate Glass with Chromium," *J. Am. Ceram. Soc.*, 68 [1] 20-24 (1985).
16. A.P. Tomsia and J.A. Pask, "Bonding of Dental Glass to Ni-Cr Alloys," *ibid.*, 69 [10] C239-240 (1986).
17. V.K. Nagesh, A.P. Tomsia and J.A. Pask, "Wetting and Reactions in the Lead Borosilicate Glass-Precious Metal Systems," *J. Mat. Sci.*, 18 [11] 2665-2670 (1983).





## PROPERTIES OF SEALS MADE WITH $\text{Li}_2\text{O}-\text{Al}_2\text{O}_3-\text{SiO}_2$ -GLASS CERAMICS AND ALUMINUM-CONTAINING AUSTENITIC STAINLESS STEELS

R. T. Cassidy and P. N. Fagin  
MRC-Mound  
Miamisburg, Ohio

### ABSTRACT

A new family of aluminum-containing austenitic stainless steels has been used to make strong, hermetic glass-ceramic to metal seals. The new alloys contain approximately 4 to 5 wt % aluminum, and are strengthened via the precipitation of a secondary hardening phase during a typical glass to metal sealing and crystallization cycle. This is unlike other stainless steels which cannot be strengthened during heat treatment and are actually weakened during glass crystallization. In this paper, data will be given on thermal expansion, alloy yield strength, metallography, hermeticity, bond strength, weldability and glass-ceramic/metal interfacial structure.

### INTRODUCTION

The manufacture of high strength pyrotechnic devices, such as actuators, requires the joining of a glass-ceramic to a metal housing and an electrical feedthrough.<sup>(1,2)</sup> These seals are required to be hermetic and strong enough to contain the high pressures associated with these devices. For the past five years, high strength, hermetic glass-ceramic to metal seals have been routinely produced at Mound<sup>(1)</sup>. This achievement has been the result of judicious material selection and a tight process control practice to ensure a uniform product.

The materials of choice for these devices have been two Ni-based superalloys and a  $\text{Li}_2\text{O}-\text{Al}_2\text{O}_3-\text{SiO}_2$  glass which can be partially crystallized (transformed into a ceramic) to achieve the desired physical and chemical properties.<sup>(1-6)</sup> Cross-sectional views of a typical glass-ceramic containing header are depicted in Figure 1 where the metallic housing and feedthroughs are separated by an insulating glass-ceramic. The housing material consists of Inconel-718\* and the electrical feedthroughs are Hastelloy C-276.\*\* The glass is phosphate nucleated and can be heat-treated to obtain the crystals that yield a high coefficient of thermal expansion necessary to match that of the metallic alloys.<sup>(6)</sup>

\*Huntington Alloy Product Div., Huntington, WV.  
\*\*Cabot Corp., Kokomo, IN.

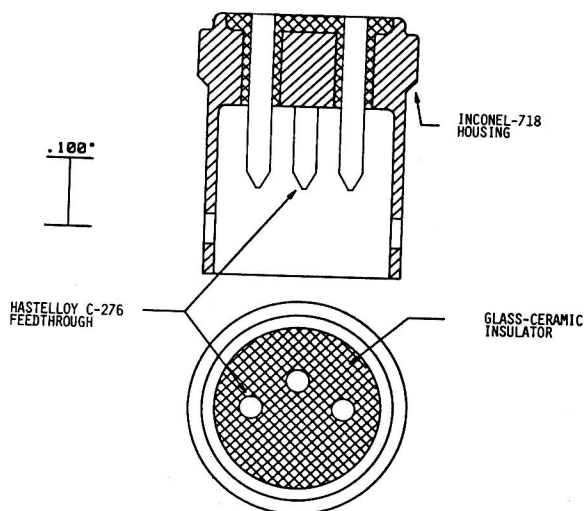


Figure 1. Cross-sectional view of a typical glass-ceramic header showing housing, metal feedthrough and glass-ceramic insulator.

#Mound is operated for the U. S. Department of Energy by Monsanto Research Corporation under contract No. DE-AC04-76-DP00053.

A typical heat-treating cycle used to seal a glass-ceramic to metal is displayed in Figure 2. Forming the seal involves a time-temperature furnace cycle which includes the first three (short cycle) or possibly all four of the following stages: 1) sealing - where the molten glass flows and bonds to the metal surface to form a hermetic seal, 2) nucleation - where crystal nuclei develop in the glass, 3) crystal growth - where the growth of the crystals which occurs on the nuclei transforms the glass into a glass-ceramic, and 4) precipitation hardening - where the metal is strengthened. A strict process control used in combination with the above material set has yielded very strong glass-ceramic to metal seals, with several designs able to withstand >100,000 psi.<sup>(5)</sup>

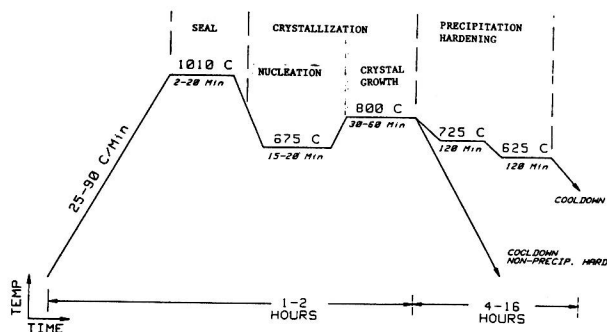


Figure 2. Typical glass-ceramic sealing/crystallization cycle with precipitation hardening.

The success of sealing the lithia-alumina-silica glass-ceramic to Inconel 718 has resulted in the pursuit of alternate material combinations that will yield a strong product. Ideally, alternate metals should be readily obtainable, low in cost, easily machineable, weldable and have coefficients of thermal expansion which are closely matched to the corresponding glass-ceramic. Candidate materials examined in this study are 304-L stainless steel, and two recently developed austenitic stainless steels that contain approximately 5 wt % aluminum<sup>(7)</sup>. This study investigates the use of these alloys as a housing material for glass-ceramic to metal seals in actuator applications. Data on metallic yield strength, bond strengths of seals, thermal expansion, weldability and glass/metal interfacial characteristics will be presented.

#### EXPERIMENTAL

Samples of two different aluminum-containing austenitic stainless steels were obtained<sup>+</sup> in the form of 0.440" thick plates or of 0.250" diameter rod. The two alloys examined are designated 896 and 899. In addition, 304-L stainless steel was obtained from Williams and Co.<sup>++</sup> in the form of 0.500" diameter rod. Table 1 shows the composition of each alloy tested.

<sup>+</sup> Samples were obtained from J. A. McGurty of the University of Cincinnati, Cincinnati, Ohio or from Hoskins Manufacturing Company of Hamburg, Michigan.  
<sup>++</sup> Cincinnati, Ohio.

Table 1 - Compositions of Alloys 896, 899 and 304-L

ALLOY	Fe	Cr	Ni	Al	C	Mn	Si
896	BAL	10.6	22.1	4.15	.03	.20	.75
899	BAL	10.6	20.9	5.2	.03	.21	.53
304-L	BAL	18-20	8-12	---	.03 (max)	2.0 (max)	1.0 (max)

Each alloy was machined to accommodate the various tests which were performed to evaluate their properties. These included standard tensile specimens for yield strength measurements<sup>(8)</sup>, cylindrical shells for hermeticity pass-fail evaluation and hydrostatic burst testing<sup>(9)</sup>, and polished cross-sections for examination of the glass-ceramic to metal interfaces with optical microscopy<sup>(10)</sup>. These experimental procedures have been described elsewhere in the listed references and will not be repeated.

Samples of alloys 896 and 899 were also tested for their susceptibility to cracks during welding. A candidate for a housing alloy must be pulsed-laser weldable, preferably to itself. Sample squares of 0.750" were machined from 0.440" thick plates of alloys 896 and 899 and electropolished<sup>(11)</sup> to remove scale from the top and bottom surfaces. Two samples of each alloy were then heat-treated to replicate the standard sealing/crystallization cycle. Following the heat-treatment, approximately 0.010" was machined from the surface to be welded and the samples were four-step cleaned<sup>(11)</sup> prior to welding.

Two weld tests known as the Weeter<sup>(12)</sup> and Deep V Groove<sup>(13)</sup> were performed. For the Weeter test, six holes were drilled in a sample plate with a 0.031" diameter bit. Two holes were drilled at three different depths (0.025", 0.030" and 0.035"). The actual weld was made by a single pulsed laser which was directed into each hole under an Argon cover gas. Pulse duration was approximately 7.5 msec. For the second test, a 0.030" deep "V" groove was machined into the alloys, the angle of the "V" being 90°. The pulse duration was 5 msec and again, an Argon cover gas was used.

A Veeco<sup>(+)</sup> helium mass spectrometer leak tester was used to ascertain hermeticity. An inner diameter of 0.150" was machined into 3/4" long samples of 1/4" diameter rod. These test pieces were then sealed using the standard short seal/crystallization cycle (i. e. nonprecipitation hardening) depicted in Figure 2. A sealed unit was considered hermetic if it was found to have a leak rate of  $\leq 10^{-8}$  cm<sup>3</sup> STP of helium per second. Three samples of alloys 896, 899 and 304-L were evaluated and found to be leak tight. The phosphate-nucleated glass<sup>++</sup> used in this study has the composition in wt% of 75.0 SiO<sub>2</sub>, 12.3 Li<sub>2</sub>O, 4.3 Al<sub>2</sub>O<sub>3</sub>, 4.2 K<sub>2</sub>O, 1.3 B<sub>2</sub>O<sub>3</sub> and 2.5 P<sub>2</sub>O<sub>5</sub>.

#### RESULTS AND DISCUSSION

The sealing of glasses to metals requires a match of their expansion coefficients, such that upon cooling 'crack-free' seals are formed. Ideally, these seals should be under a slight compression after cooling, so that a tight fit of metal (housing) around the glass or the glass around the metal (feedthrough) is assured. In addition, the metal should be compatible with the hot glass at the sealing temperature. The hot glass should not attack the metal and produce reaction products that develop voids or pores, which can destroy the hermeticity and strength of a seal.

<sup>+</sup> Model MS-20, Plainview, NY 11803.  
<sup>++</sup> Glass cylinders were obtained from Schott Glass Technologies, Duryea, PA and were centerless ground to a 0.140 ± 0.001" diameter.

Figure 3 depicts the thermal expansion coefficients of Inconel 718 and the three "alternative" materials examined in this study, 304-L and alloys 896 and 899. A plot of the thermal expansion characteristics for the  $\text{Li}_2\text{O}-\text{Al}_2\text{O}_3-\text{SiO}_2$  glass-ceramic has also been included. The two aluminum-containing alloys have similarly "high" expansion coefficients when compared to Inconel 718 and 304-L. A closer examination of Figure 3 reveals that both aluminum-containing alloys, 896 and 899, have lower thermal expansions than 304-L, the significance of which is that these new alloys are more closely matched (than 304-L) to the presently used glass ceramic. Therefore, a seal made between these new alloys and the lithia-alumina-silica glass-ceramic will result in the glass being under compression.

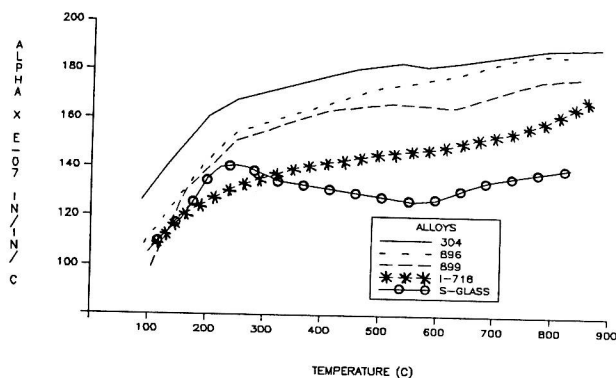


Figure 3. Thermal expansion coefficients of housing materials (Inconel 718, 304-L, 896 and 899) and of glass-ceramic.

One of the design criteria for a glass ceramic containing actuator is that the metallic component possess a high yield strength. Figure 4 illustrates the yield strengths of Inconel 718 and candidate housing materials, 304-L and 896. Values were determined for the metals in both the as-received condition and after they were subjected to the seal/crystallization cycle (Figure 2). Yield strength data are also included for alloy 896 that had witnessed additional heat treatments immediately following the seal/crystallization cycle; these consisted of 1), a two hour hold at 610°C and 2), a ten hour hold at 610°C. Results indicate that the yield strength of alloy 896 is improved following a standard seal/crystallization cycle, whereas 304-L is actually weakened. Moreover, alloy 896 can be further strengthened if additional heat treatments are included. The ten-hour soak at 610°C resulted in a yield strength of 84 KSI. As a comparison, Kovar, following a standard glass sealing cycle, has a yield strength of ca 40 Ksi. Previous work has revealed that alloy 896 can be heat-treated to achieve a yield strength in excess of 100 KSI. (7).

The microstructures of alloy 896 in the as-received and post-sealed conditions are depicted in Figures 5(a) and 5(b), respectively. It is evident that the post sealed sample contains a dark secondary phase, approximately 5 to 10 microns in size, which is primarily located at the grain boundaries. This secondary phase is not as prevalent in the as-received sample. Wavelength dispersive x-ray analysis was performed on this phase in the post-sealed sample and revealed its composition to be primarily  $\text{NiAl}$ . This analysis agrees well with earlier work (7) which also noted the presence of this secondary phase. These results indicate that a seal/crystallization cycle, with no additional heat treatment, has improved the microstructure of alloy 896 via precipitation of the toughening  $\text{NiAl}$  phase. This accounts for the increase in yield strength seen in Figure 4.

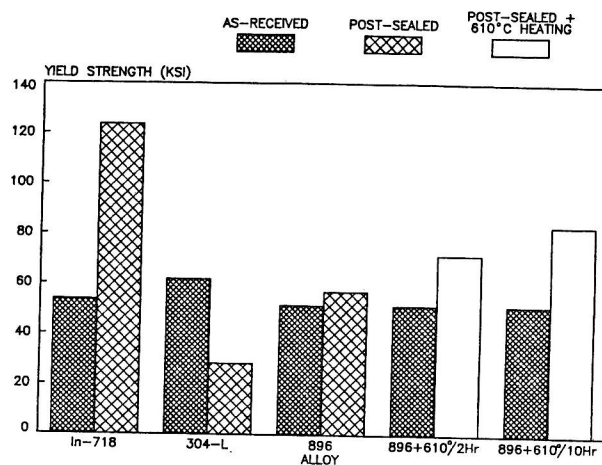


Figure 4: Yield strength data for Inconel 718, 304-L, and 896 alloys in the as-received and post-sealed states.

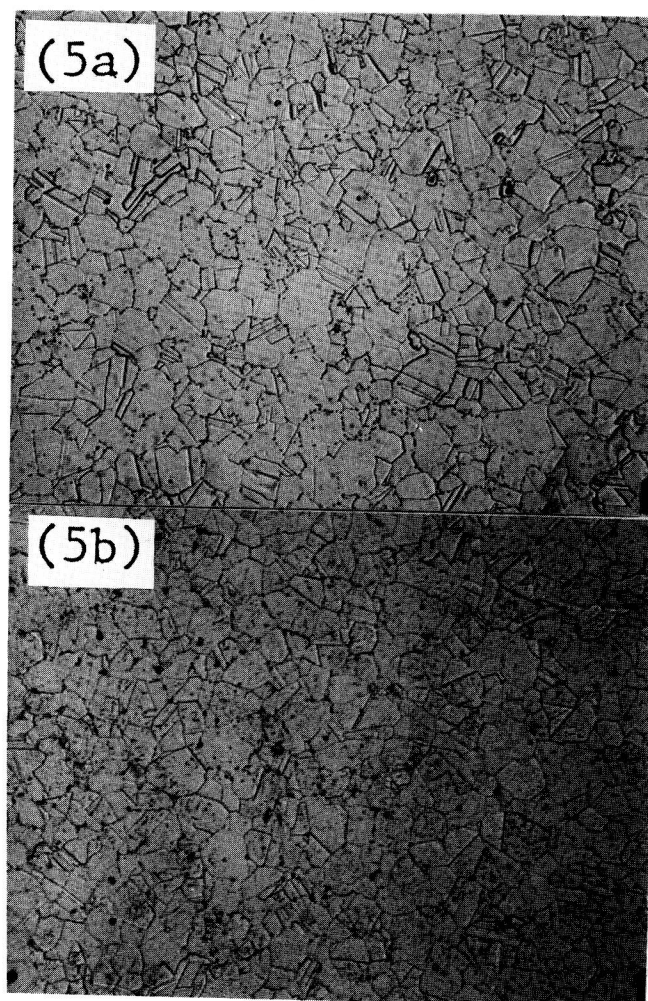


Figure 5: Microstructure of alloy 896 as-received (5a) and after a seal/crystallization cycle (5b). (500X)



For the purpose of obtaining glass-ceramic to metal bond strengths, test shells (depicted in Figure 6) were machined from one of the aluminum-containing alloys (896), and Inconel 718. Following a standard four-step cleaning process, the shells were loaded with glass and subjected to the seal/crystallization cycle. The sealed units were then machined to a constant glass depth and their bond strength was determined by measuring the hydrostatic force necessary to shear the glass plug out of the unit. The average bond strength values determined for ten (10) samples were 5200 psi ( $\sigma \pm 245$ ) for alloy 896 and 3400 psi ( $\sigma \pm 500$ ) for Inconel 718. The results for Inconel 718 agree with other published values. (9)

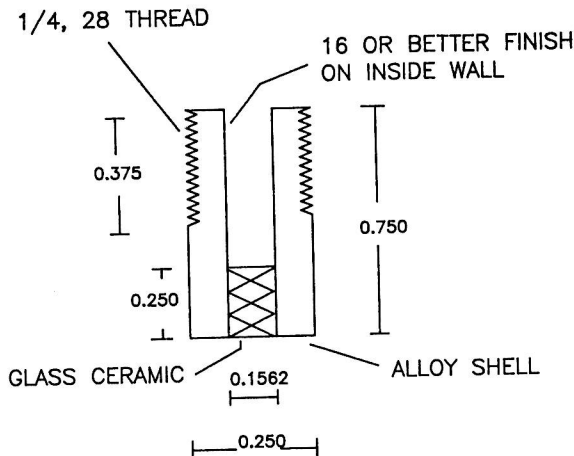


Figure 6: Test shell used to determine glass-ceramic to metal (Inconel-718 and 896) bond strength.

The significant difference seen in the glass/metal bond strengths between these two metals can be explained in terms of the greater compressive stress developed by alloy 896 during sealing. This increase in compression is due to the alloy's larger coefficient of thermal expansion when compared to Inconel 718. To prove this theory, additional 1/4" dia test shells were machined with a larger inside diameter (0.179" vs 0.150"), and thus a smaller wall thickness (.035" vs .050"). If the higher coefficient of thermal expansion is causing greater "squeezing" of the glass-ceramic in the alloy 896, then a thinner-walled test shell would yield a lower bond strength as measured in this test. The results of the additional test revealed that the thinner-walled alloy 896 test shells had a burst strength of 4000 psi ( $\sigma \pm 269$ ), a decrease of greater than 20 % when compared

to the thick-walled results. The Inconel 718 results essentially remained the same, 3500 psi ( $\sigma = \pm 817$ ). The significance of this second test is that although the 896 alloy has vastly improved bond strengths when compared to Inconel 718, it might, at least partially, be due to a greater compressive stress or squeezing of the glass than a direct measurement of chemical bond strength.

Prior to this study, minimal weld testing had been performed on the aluminum-containing alloys. Previous work, carried out at ORNL (7), found both alloy 896 and 899 to be weldable with electron beam or gas-tungsten arc welding. However, no previous laser weld studies have been performed on these alloys to our knowledge.

To test these new alloys for their ability to be welded with a YAG laser, both alloys 896 and 899 were subjected to the Weeter weldability test. This test consists of a single laser directed into a drilled hole. Test results indicate that alloy 899 is pulse laser weldable and that alloy 896 is very crack sensitive.

To further evaluate alloy 899, the more severe deep "V" groove test (13) was used. The micrographs depicted in Figures 7a and 7b show the results of this test on Alloy 899; these micrographs are 100X transverse optical cross-sections (polished and etched) of low and high powered pulsed-laser welds, respectively. No cracks can be observed in this view and magnification. Additional grinding and polishing down through the welds revealed no cracks to be present. The micrographs illustrated in Figures 7c and 7d are longitudinal cross-sections of the welds, again for low and high powered pulses, respectively. Small cracks can be noted in both specimens. As a comparison, an identical test carried out on Inconel-718 in previous work indicates that alloy 899 is less crack sensitive than Inconel 718. (13) Therefore, it can be concluded that alloy 899 is laser weldable for applications in actuators.

